

PAPER • OPEN ACCESS

## Identification of low-energy isovector octupole states in $^{144}\text{Nd}$

To cite this article: M Thürauf *et al* 2016 *J. Phys.: Conf. Ser.* **724** 012050

View the [article online](#) for updates and enhancements.

### Related content

- [Octupole shapes](#)  
P A Butler
- [Isoscalar and isovector spin-flip M1 strengths in  \$^{11}\text{B}\$](#)   
T Kawabata and the RCNP E114, E137 and E207 Collaborations
- [Dynamical Structure of Nuclear Excitation in Continuum](#)  
Zhang Chun-Lei, Zhang Huan-Qiao and Zhang Xi-Zhen

### Recent citations

- [EXILL—a high-efficiency, high-resolution setup for -spectroscopy at an intense cold neutron beam facility](#)  
M. Jentschel *et al*

# Identification of low-energy isovector octupole states in $^{144}\text{Nd}$

**M Thürauf<sup>1</sup>, M Scheck<sup>1,2,3</sup>, C Bernards<sup>4</sup>, A Blanc<sup>5</sup>, N Cooper<sup>4</sup>, G Defrance<sup>6</sup>, M Jentschel<sup>5</sup>, J Jolie<sup>7</sup>, O Kaleja<sup>1</sup>, U Köster<sup>5</sup>, T Kröll<sup>1</sup>, P Mutti<sup>5</sup>, G S Simpson<sup>8</sup>, T Soldner<sup>5</sup>, M Tezgel<sup>1</sup>, W Urban<sup>9</sup>, J Vanhoy<sup>10</sup>, M Werner<sup>1</sup>, V Werner<sup>1,4</sup>, and K O Zell<sup>7</sup>**

<sup>1</sup> Institut für Kernphysik, TU Darmstadt, Schlossgartenstr. 9, 64289 Darmstadt, Germany

<sup>2</sup> School of Eng. and Comp., Univ. of the West of Scotland, High Street, Paisley PA1 2BE, UK

<sup>3</sup> The Scottish Universities Physics Alliance, University Avenue, Glasgow G12 8QQ, UK

<sup>4</sup> Wright Laboratory, Yale Univ., P.O. Box 208120, New Haven, CT 06520-8120, USA

<sup>5</sup> Institut Laue-Langevin, 71 avenue des Martyrs, 38000 Grenoble, France

<sup>6</sup> Grand Accélérateur National d'Ions Lourds, Boulevard Henri Becquerel, 14000 Caen, France

<sup>7</sup> Institut für Kernphysik, Universität zu Köln, Zülpicher Str. 77, 50937 Köln, Germany

<sup>8</sup> LPSC, UJF Grenoble I, 53 avenue des Martyrs, 38026 Grenoble Cedex, France

<sup>9</sup> Faculty of Physcis, University of Warsaw, ul. Pasteura 5, 02-093 Warsaw, Poland

<sup>10</sup> Dep. of Physics, U.S. Naval Academy, 121 Blake Road, Annapolis, MD 21402, USA

E-mail: [mthuerauf@ikp.tu-darmstadt.de](mailto:mthuerauf@ikp.tu-darmstadt.de)

**Abstract.** Recently, first candidates for low-lying isovector states in the octupole sector were suggested. The unambiguous identification of those states will contribute to the decomposition of the octupole-octupole residual interaction in an isoscalar and isovector part. This will help us understand the octupole degree of freedom. In  $^{144}\text{Nd}$  the  $3^-$  state at 2778 keV is a good candidate for such a “mixed-symmetry” octupole state. In order to clarify the nature of this state, a  $^{143}\text{Nd}(n, \gamma)$ -experiment was conducted with the EXILL-setup. Following neutron capture the  $3^-$  states are populated and EXILL provides the opportunity to determine the multipole-mixing ratios of the  $3_i^- \rightarrow 3_1^-$  transitions. For the transition from the “mixed-symmetry” octupole state to the symmetric  $3_1^-$  state we expect a strong  $M1$  component.

## 1. Introduction

Low-energy isovector states like the  $1^+$  scissors mode [1–5] in deformed nuclei or the mixed-symmetric  $2^+$  states [6, 7] in near-spherical nuclei are well established in those nuclei. In contrast to quadrupole mixed-symmetry states, octupole mixed-symmetry states are known only sparsely in the present time, but are predicted by the sdg-IBA-2 [8]. First experimental evidence was found through an enhanced  $3_i^- \rightarrow 3_1^- M1$ -transition in  $^{94}\text{Mo}$  [9]. More recently, candidates for isovector octupole states were suggested from additional  $(n, n'\gamma)$  data on  $^{92}\text{Zr}$ ,  $^{96}\text{Mo}$  and  $^{144}\text{Nd}$  [10] supported also from charged particle scattering data [11]. The proof of the existence of isovector octupole states in these nuclei will help us to understand the octupole degree of freedom and the interaction of protons and neutrons in atomic nuclei. In the present work the first results for  $^{144}\text{Nd}$ , populated via cold-neutron capture, are presented.



Content from this work may be used under the terms of the [Creative Commons Attribution 3.0 licence](https://creativecommons.org/licenses/by/3.0/). Any further distribution of this work must maintain attribution to the author(s) and the title of the work, journal citation and DOI.

### 1.1. Mixed-symmetry states

The concept of mixed-symmetry states is defined in the framework of the Interacting Boson Model version 2 (IBM-2) [12]. The basic idea of this model is the coupling of the valence protons and neutrons to *s*-, *d*- and in our case to *f*-bosons (sdf-IBM-2 [8]). The isospin analogue in the IBM formalism is the *F*-spin concept: Protons and neutrons have  $F = \frac{1}{2}$  with projections  $F_z = +\frac{1}{2}$  for protons and  $F_z = -\frac{1}{2}$  for neutrons. The wavefunction of a state with maximum *F*-spin  $F = F_{\max} = \frac{1}{2}(N_{\pi} + N_{\nu})$  behaves symmetric under pairwise exchange of proton and neutron bosons, where  $N_{\rho}$  are the numbers of proton and neutron bosons ( $\rho \in \{\pi, \nu\}$ ). This class of states is called fully-symmetric states (FSS).

States with  $F$ -spin  $F < F_{\max}$  are mixed-symmetry states (MSS) and a part of their wavefunction behaves anti-symmetric under proton and neutron boson exchange. Usually the mixed-symmetry states in vibrational nuclei and the scissors mode in deformed nuclei are states with  $F = F_{\max} - 1$ . The IBM *M1*-Operator is given by [7]:

$$T(M1) = \sqrt{\frac{3}{4\pi}} \left[ \frac{N_{\pi} g_{\pi} + N_{\nu} g_{\nu}}{N} L_{\text{tot}} + (g_{\pi} - g_{\nu}) \frac{N_{\pi} N_{\nu}}{N} \left( \frac{L_{\pi}}{N_{\pi}} - \frac{L_{\nu}}{N_{\nu}} \right) \right] \mu_N, \quad (1)$$

where  $g_{\rho}$  are the *g*-factors and  $N$  the total number of the constituent bosons.  $L_{\rho}$  denotes the angular momentum operator for proton and neutron bosons. It can be shown, that *M1* transitions from FSSs to FSSs are forbidden, but allowed for transitions from MSSs to FSSs, which can be used as an experimental signature for these class of states: For a octupole MSS we expect a strong *M1* transition with  $\langle 3_{\text{FSS}} | T(M1) | 3_{\text{MSS}} \rangle \approx 1 \mu_N$  and a weak *E3* of a few single particle units for  $3_{\text{MSS}}^- \rightarrow 0_{\text{gs}}^+$ .

## 2. Experiment

The EXOGAM Ge detector array was placed at the cold-neutron beam line PF1B at the Institut Laue-Langevin (ILL) in Grenoble, France. The cold neutrons generated in a high-flux reactor were collimated so that the beam had a diameter of 12 mm and a flux of  $\Phi = 10^8 \frac{1}{\text{s cm}^2}$  at the target position. The target was positioned in the center of a frame, where eight EXOGAM clover HPGe-detectors were mounted at  $90^\circ$  with respect to the beam axis. The capsules of the EXOGAM detectors were surrounded with an active anti-Compton shield (BGO) to reduce the Compton background. A detailed description of the experimental setup can be found in Refs. [13, 14] and references therein.

In our case the target (0.8 mg) was enriched to 91 % in  $^{143}\text{Nd}$ , which has a  $(n, \gamma)$  cross section of 330 b for thermal neutrons. The combination of high thermal neutron-capture cross section and the enrichment of the target made it possible to conduct the experiment in one day with sufficient statistics. For calibration a  $^{152}\text{Eu}$  source was placed at the target position before and after the Nd-runs. The daughters of  $^{152}\text{Eu}$ ,  $^{152}\text{Gd}$  and  $^{152}\text{Sm}$ , have well known  $\gamma$ -ray intensities and energies, as well as multipole-mixing ratios.

The data acquisition system was run in triggerless timestamped mode so that every hit of a  $\gamma$  ray was written as an event to the data stream. This required the implementation of a new eventbuilder which can read and sort the  $\gamma$  events. The eventbuilder is able to identify  $\gamma$  rays which were in coincidence with each other and, if there were any, with the corresponding BGO events. On top of this eventbuilder an addback-algorithm for the clover-detectors was implemented to reduce the loss of full-energy events due to the Compton effect.

## 3. Analysis

### 3.1. Angular correlations

The eight EXOGAM-clover-HPGe detectors can be used for angular-correlation measurements. The octagonal construction of the frame gives us the opportunity to measure correlations between

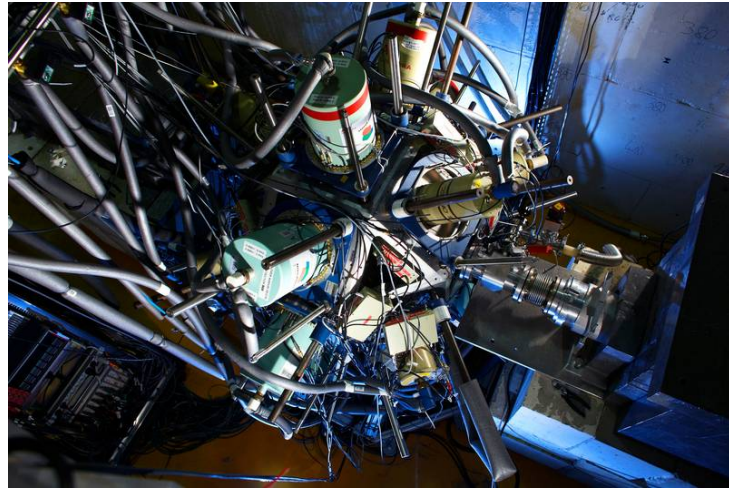


**Figure 1.** EXOGAM setup at the cold-neutron beam line PF1B at ILL. The neutrons enter from the right side impinging on a target (here  $^{143}\text{Nd}$ ) in the center of the frame. One can see the eight EXOGAM-clover-HPGe detectors perpendicular to the beam axis which are used for the angular-correlation measurement in this work.

four angular groups:  $45^\circ$ ,  $90^\circ$ ,  $135^\circ$  and  $180^\circ$ . From the angular correlation measurement the transmitted angular momentum  $l$  of the  $\gamma$  radiation and the multipole-mixing ratio  $\delta$  can be extracted. A detailed description of angular correlation techniques can be found in Ref. [15–17].

In experiments with thermal- or cold-neutrons the neutron beam doesn't characterize a  $z$ -axis of the quantum system like it would be in Coulomb excitation or  $(\gamma, \gamma')$  reactions. The angular distribution of  $\gamma$  rays after thermal- and cold-neutron capture is isotropic with respect to the neutron beam axis. To obtain a non-isotropic distribution of magnetic substates,  $\gamma$ - $\gamma$ -matrices have to be sorted and a gate is set on the populating or depopulating transition. Subsequently the peak volumes of the depopulating or populating transition can be determined, which shows now a non-isotropic distribution with respect to the direction of the emitted (de)populating  $\gamma$  ray.

Angular correlations  $\tilde{W}(\theta)$  can be parameterized as

$$\tilde{W}(\theta) = 1 + A_2 P_2(\cos \theta) + A_4 P_4(\cos \theta) \quad (2)$$

where  $A_{\{2,4\}}$  are the correlation coefficients and  $P_{\{2,4\}}(x)$  the Legendre polynomials of 2<sup>nd</sup> and 4<sup>th</sup> order. Usually the normalization of the experimental data is done with respect to the  $90^\circ$  angular group:

$$W(\theta) = \frac{\tilde{W}(\theta)}{\tilde{W}(90^\circ)} = \frac{1 + A_2 P_2(\cos \theta) + A_4 P_4(\cos \theta)}{1 - \frac{1}{2}A_2 + \frac{3}{8}A_4}. \quad (3)$$

For each  $\gamma$ -ray cascade the  $A_k$  can be calculated analytically depending on the spin of each state in the cascade and the  $\delta$  of the first or the second transition. The experimental values of  $A_k$  have to be corrected by attenuation factors  $Q_k$ , which can be determined from a well-known cascade e.g. 0–2–0 cascades, because here we have a strong angular correlation ( $A_2^{\text{theo.}} = 0.3571$ ,  $A_4^{\text{theo.}} = 1.1429$ ) and no  $\delta$  is involved.

In general, the number of detector combinations is not the same for each angular group. In our case we have eight pairs in the  $45^\circ$ ,  $90^\circ$  and  $135^\circ$  groups, but only four pairs in the  $180^\circ$  group. To correct for this varying number and consider eventual differences in the absolute detection efficiency a 2–0–2 cascade was used for normalization. Owing to the reaction mechanism of

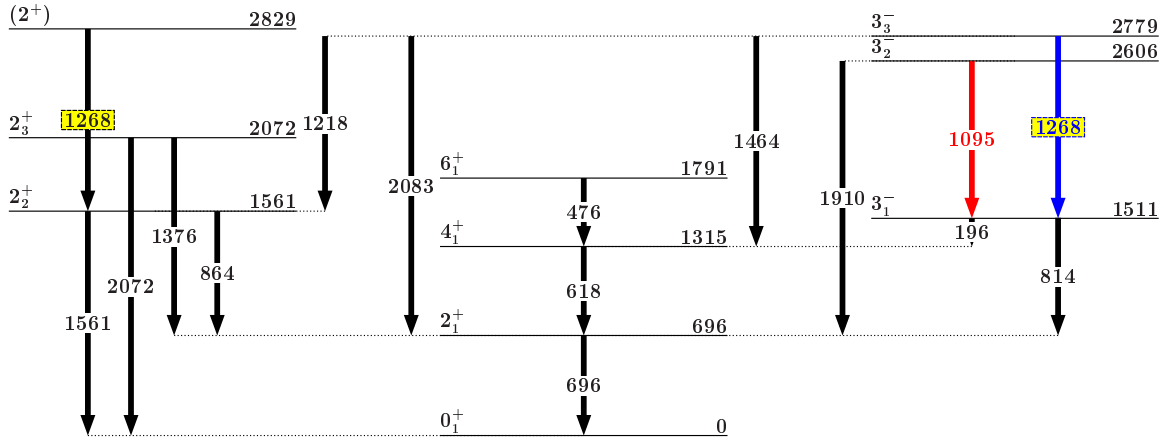


**Figure 2.** Partial level scheme of  $^{144}\text{Nd}$ . The red and blue colored transitions are the transitions of interest for this work.

the  $^{143}\text{Nd}(n, \gamma)$  reaction  $0^{+,-}$  states are populated only weakly and cascades involving them are unsuitable. Consequently a calibration source had to be employed.

### 3.2. Multipole-mixing ratio

In this work the definition of the multipole-mixing ratio from Ref. [18] and the references therein is used:

$$\delta = \frac{\sqrt{3}}{10} \frac{E_\gamma}{\hbar c} \frac{\langle J_f || \hat{M}(E2) || J_i \rangle}{\langle J_f || \hat{M}(M1) || J_i \rangle}, \quad (4)$$

where  $\hat{M}$  is the electro-magnetic multipole operator for  $E2$  and  $M1$  radiation. For the phase convention the definition of Krane and Steffen [17] is used. Determining multipole-mixing ratios via angular correlations is a necessity to identify mixed-symmetric states. For cascades with competing  $M1$  and  $E2$  transitions the  $A_k$  coefficients become functions of  $\delta$ .

In  $^{152}\text{Sm}$  the  $3_1^+$  state is populated via the electron capture of  $^{152}\text{Eu}$ . This  $3^+$  state decays predominantly via  $M1$  or  $E2$  transitions to the  $4_1^+$  and the multipole-mixing ratio is well known from literature ( $\delta(3_1^+ \rightarrow 4_1^+) = -6.5(3)$  [19]). Placing a gate on the 868-keV transition  $4_1^+ \rightarrow 2_1^+$  and fitting the angular correlation function with  $\delta$  as a free parameter leads to a  $\chi^2$ -minimum at  $\delta = -6.2$  which is in agreement with the literature value.

### 3.3. Octupole transitions in $^{144}\text{Nd}$

Hicks *et al.* [20] conducted a  $(n, n'\gamma)$  experiment at the University of Kentucky Accelerator Laboratory in Lexington, USA, in order to clarify spectroscopic uncertainties in  $^{144}\text{Nd}$ . The original assignment of the  $3_3^-$  state as a candidate for a mixed-symmetric octupole state is based on this dataset [10]. The major problem with this experiment was that the 1268-keV peak is a doublet consisting of transitions from  $(2_x^+) \rightarrow 2_2^+$  ( $E(2_x^+) = 2829$  keV) and  $3_3^- \rightarrow 3_1^-$  which cannot be separated in single  $\gamma$ -ray spectroscopy (see level scheme Fig. 2). To clarify the nature of the  $3_3^-$  state the experiment at ILL was performed.

It was shown by Robinson *et al.* that the  $3_2^-$  state at 2606 keV is not a mixed-symmetry state but member of the quadrupole-octupole-quintuplet  $[|2_x^+ \rangle \otimes |3_1^- \rangle]_{3-}$  [21]. This fact was confirmed by Hicks *et al.* as well. Here a strong  $B(E2)$  strength of 23(4) W.u. and a weak  $B(M1)$  of  $7.0(13) \times 10^{-3} \mu_N^2$  for the  $3_2^- \rightarrow 3_1^-$  transition was measured.

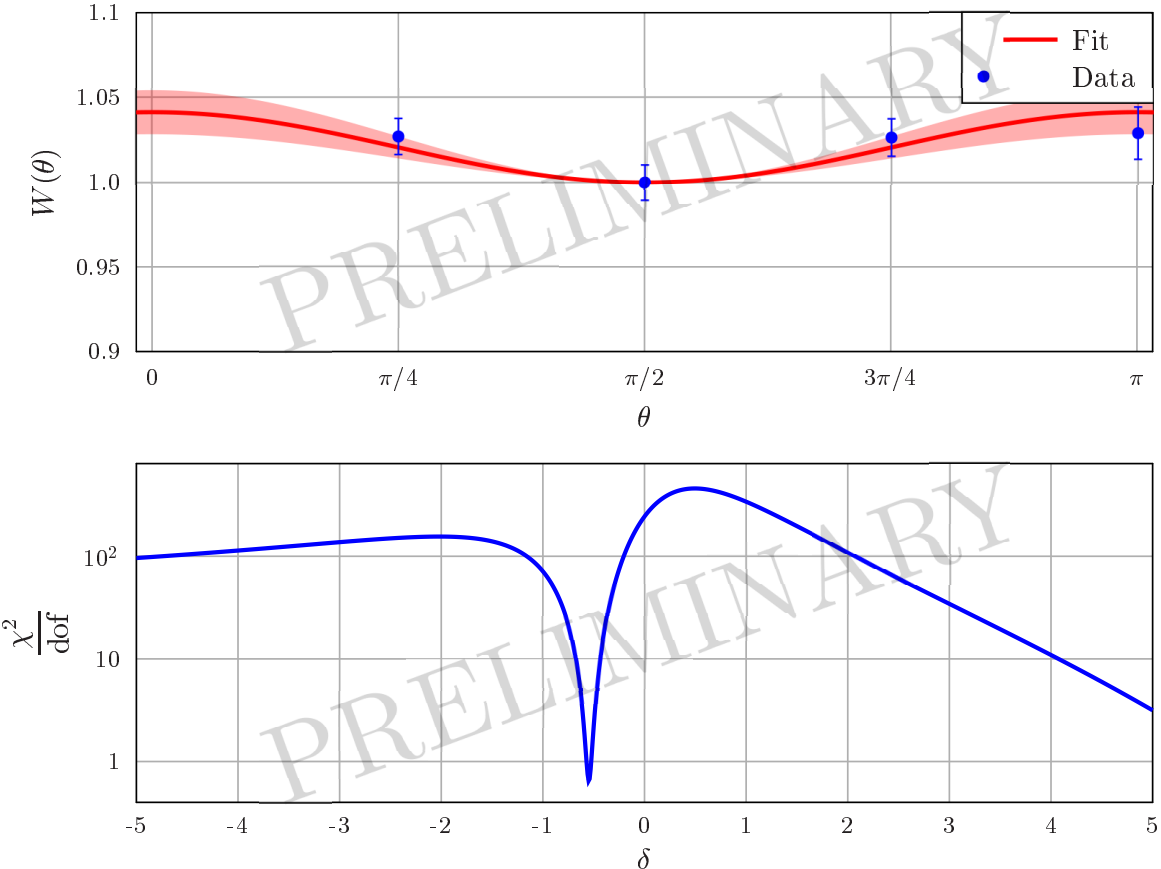


**Figure 3.** The upper figure shows the fitted angular correlation function to the data points of the  $3_3^- \rightarrow 3_1^- \rightarrow 2_1^+$  cascade in  $^{144}\text{Nd}$ . The lower picture shows the reduced  $\chi^2$  distribution of this fit with a pronounced minimum at  $\delta = -0.55$ .

In this work we apply angular-correlation techniques to precisely determine the multipole-mixing ratio  $\delta(3_3^- \rightarrow 3_1^-)$ . The capture state  $(\frac{7}{2}(f_{7/2}) \pm \frac{1}{2}(n))$  of  $^{144}\text{Nd}$  is a  $3^-$  or  $4^-$  state and the  $3_3^-$  is populated either directly by a  $M1/E2$  transition with an unknown multipole-mixing ratio or via unknown intermediate states. Therefore, as a gate to separate the  $3_3^- \rightarrow 3_1^-$  transition from the contaminating transition the  $3_1^- \rightarrow 2_1^+$ - $E1$ -transition at 814 keV is favourable. This transition is of pure  $E1$  character. Consequently, for each value of  $\delta(3_3^- \rightarrow 3_1^-)$  in this cascade,  $A_4$  equals to zero, and the ellipse in the  $A_2$ - $A_4$ -space corresponding to the different  $\delta$  becomes a string. This results in two minima in the  $\chi^2$  plot with comparable  $\chi^2$  values.

In Fig. 3 the fitted angular correlation function to the data points and the  $\chi^2$  distribution is shown. The  $\chi^2$  distribution shows a minimum at  $\delta = -0.55$  which is a strong indicator for the  $3_3^-$  state to be a mixed-symmetric octupole state. Table 1 shows an overview of all multipole-mixing ratios determined so far with the current  $(n, \gamma)$  dataset.

#### 4. Outlook

In order to get the absolute  $B(M1; 3_3^- \rightarrow 3_1^-)$  strengths in  $^{144}\text{Nd}$  the collaboration intends to measure the lifetime of the  $3_3^-$  state. The lifetime of states which decay via strong dipole transitions is settled in the femtosecond range. A suitable setup for such a lifetime measurement especially with non-Yrast-states is the high-resolution flat-crystal  $\gamma$ -ray facility, GAMS, at ILL,

**Table 1.** Overview of preliminary multipole-mixing ratios  $\delta$  determined with the current  $^{143}\text{Nd}(n, \gamma\gamma)$  dataset.

	This work	D.M. Snelling <i>et al.</i>	S.F. Hicks <i>et al.</i>
$\delta(2_2^+ \rightarrow 2_1^+)$	-0.94	$-1.13_{-2}^{+15}$	$-0.93_{-523}^{+30}$
$\delta(2_3^+ \rightarrow 2_1^+)$	0.19	$0.31_{-9}^{+11}$	$0.6_{-3}^{+4}$
$\delta(4_2^+ \rightarrow 4_1^+)$	-0.3		$-0.5_{-5}^{+8}$
$\delta(3_1^+ \rightarrow 2_1^+)$	0.45		$0.8_{-4}^{+9}$
$\delta(3_2^- \rightarrow 3_1^-)$	-2.0		$-3_{-13}^{+3}$
$\delta(3_3^- \rightarrow 3_1^-)$	-0.55		$-0.37_{-11}^{+18}$

where it will be possible to separate also the energy doublet at 1268 keV in  $^{144}\text{Nd}$ .

### Acknowledgments

This work is supported by the Deutsche Forschungsgemeinschaft through Grant No. KR 1796/2-1, BMBF Grand No. 05P12RDFN8, U.S. Department of Energy Grand No. DE-FG02-91ER-40609 and HGS-HIRe for FAIR. M. Scheck acknowledges financial support from the STFC. Financial support by the ILL to realize the fantastic opportunity of EXILL is gratefully acknowledged.

### References

- [1] Indice N L and Palumbo F 1978 *Phys. Rev. Lett.* **41** 1532
- [2] Richter A 1983 *Proc. of the Int. Conf. on Nuclear Physics*
- [3] Iachello F and Arima A 1987 *The Interacting Boson Model* (Cambridge University Press)
- [4] Caprio M A and Iachello F 2005 *Annals of Physics* **318** 454
- [5] Heyde K, von Neumann-Cosel P and Richter A 2010 *Reviews of Modern Physics* **82** 2365
- [6] Iachello F 1984 *Phys. Rev. Lett.* **53** 1427
- [7] Pietralla N, von Brentano P and Lisetskiy A F 2008 *Progress in Particle and Nuclear Physics* **60** 225
- [8] Smirnova N A, Pietralla N, Mizusaki T and van Isacker P 2000 *Nucl. Phys. A* **678** 235
- [9] Fransen C *et al.* 2003 *Phys. Rev. C* **67** 024307
- [10] Scheck M, Butler P A, Fransen C, Werner V and Yates S W 2010 *Phys. Rev.* **81** 064305
- [11] Scheck M 2012 Experimental evidences for low-lying octupole isovector states *Journal of Physics: Conference Series* vol 366 p 012040
- [12] Arima A, Ohtsuka T, Iachello F and Talmi I 1977 *Physics Letters B* **66** 205
- [13] Jentschel M *et al.* *Journal of Instrumentation* to be submitted
- [14] Jolie J *et al.* 2015 The  $(n, \gamma)$  campaigns at exill *EPJ Web of Conferences* vol 93 p 01014
- [15] Frauenhlder H and Steffen R M 1965 *Alpha-, Beta-, and Gamma-Ray Spectroscopy* (North-Holland Publishing Company)
- [16] Urban W *et al.* 2013 *Journal of Instrumentation* **8** P03014
- [17] Krane K S, Steffen R M and Wheeler R M 1973 *Nucl. Data Tables* **11** 351
- [18] Stahl C, Pietralla N, Rainovski G and Reese M 2015 *Nuclear Instruments & Methods in Physics Research A* **770** 123
- [19] Lange J, Kumar K and Hamilton J H 1982 *Reviews of Modern Physics* **54** 1982
- [20] Hicks S F, Davoren C M, Faulkner W M and Vanhoy J R 1998 *Phys. Rev. C* **57** 2264
- [21] Robinson S J *et al.* 1999 *Physics Letters B* **465** 61